Lawrence Berkeley National Laboratory

Title
The Luminosity Monitoring System for the LHC: Modeling and Test Results

Permalink
https://escholarship.org/uc/item/57d0q6qd

Author
Ratti, A.

Publication Date
2010-05-28

Peer reviewed

The Luminosity Monitoring System for the LHC: Modeling and Test Results

A. Ratti*, J. F. Beche*, J. Byrd*, K. Chow*, P. Denes*, L. Doolittle*, W. Ghiorso*, P. F. Manfredi*, H. Matis*, M. Monroy*, D. Plate*, T. Stezelberger*, J. Stiller*, B. Turko*, W. C. Turner*, H. Yaver*, S. Zimmermann*, E. Bravin‡, A. Drees†, R. Miyamoto†

Abstract—Simulation results of the *Beam Rate of Neutrals* (BRAN) luminosity detector for the CERN Large Hadron Collider are presented. The detectors are intended to measure the bunch-by-bunch relative luminosity at the *ATLAS* and *CMS* experiments. Building up from experimental results from test runs at the SPS, RHIC and ALS we extend the simulated setup to the *TAN* neutral absorbers located at 140 m at both sides the IP1 and IP5 interaction points. The expected signal amplitudes are calculated for *pp*-collisions energies between 450 GeV and 7 TeV using the Monte Carlo package *FLUKA* and its graphical user interface *FLAIR*.

I. Introduction

THE BRAN luminosity detectors measure the rate of neutrals produced per *pp* interaction in the Interaction Points IP1 and IP5 of the collider. The neutrals produce Minimum Ionizing Particle (MIPs) showers in the TAN absorbers located at 140m each side of the Interaction Points. The signal from the shower is proportional to the rate of neutral particles and hence to the luminosity. For their nature the BRAN detectors provide a *relative* luminosity information. Their main application is to provide a tool for the control of the bunch overlap at a given IP (vernier scans) thus contributing to the optimization of the luminosity. The detectors are comprised of gas ionization chambers installed in slots of the TAN absorbers at a depth where the shower is expected to reach its maximum and the luminosity is estimated from a measurement of the energy released in the detectors. The choice of a four quadrant segmentation provides additional information on the beam crossing angle and the bunch sizes in collision. This paper describes the final design of the device which saw first signals from the early beam commissioning run in 2008 and is ready to operate in 2009.

II. Design Criteria

The BRAN detector consists of four quadrants each segmented into six pressurized gas gaps. Each quadrant covers an area of 4×4 cm providing a total active area of 64 cm^2. An exploded view of the detector is shown in Fig. 1.

In order to provide a bunch-by-bunch luminosity measurement the monitoring system is designed for pulsed operation which sets the requirement for an operational speed compatible with the LHC 40MHz bunch crossing rate.

The detectors must stand an extremely high radiation dose (up to 1 GGy) before a replacement is possible, a dose exceeding by at least two orders of magnitude that anticipated for the detectors in LHC experiments. The gas ionization chamber was designed adopting a combination of ceramic and metallic materials selected for their radiation hardness properties. The sensitive volume of the chamber is subdivided into thin gaps to reduce the traveling path of the charged carriers. The gas mixture must feature an adequately high electron drift velocity without using organic molecules that may polymerize under the effect of radiation. We opted for a mixture of Argon and Nitrogen.
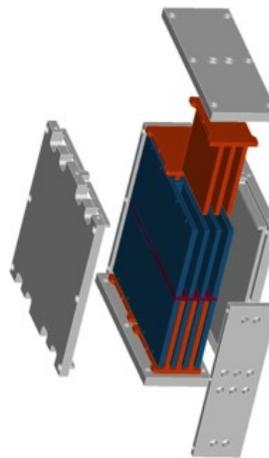

Figure 1. Exploded view of the ionization chamber. Shown are the ceramic cover (grey), the grounded Copper plates (red) and the Copper plates (blue).

The requirements for the front end electronics are also stringent. The noise issues are not trivial because the response of the analog channel to a δ-function impulse detector current must have a peaking time of a few nanoseconds as required by the LHC 25ns bunch spacing. A suitable dynamic range is required as the system must be able to detect from a minimum of one up to about 20 *pp* interactions per bunch crossing. Fluctuations in the energy deposited by the shower may actually extend the range beyond these limits. Finally the harsh radiation environment sets constraints on the choice of the electronics components.

III. Detector Characterization

In preparation for the LHC operation the detector performance has been modeled using the code FLUKA and tested with beam at the RHIC, the ALS and the CERN SPS.

A. Beam tests at the ALS

The test facility at the ALS booster allows for single bunch testing at 1Hz repetition rate . This test is instrumental for the validation of the computer modeling. We have been able to characterize the detector's position sensitivity, as well as its response to changes in the gas mixture (Fig. 2) and pressure, or to the applied bias voltage.
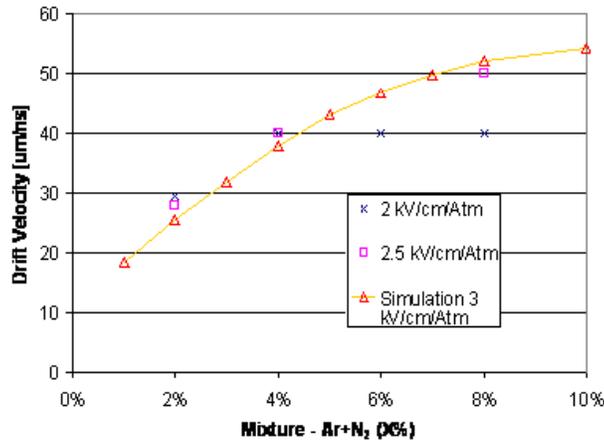

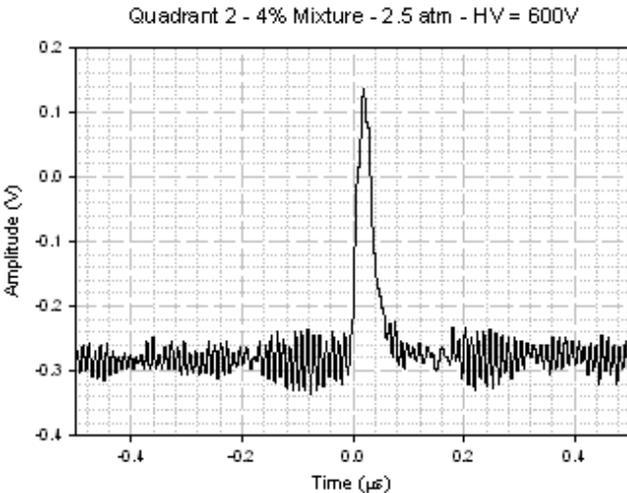Figure 2.   Simulated and measured chamber drift velocity.

Figure 3.   Typical signal from ALS beam pulse

Using the 40 MHz ALS filling pattern and the slow beam spill technique we verified the high speed performance of the detector and of the front-end electronic. Fig. 3 shows the device response to a single beam pulse while Fig. 4 shows the response to a 25ns bunch spacing.
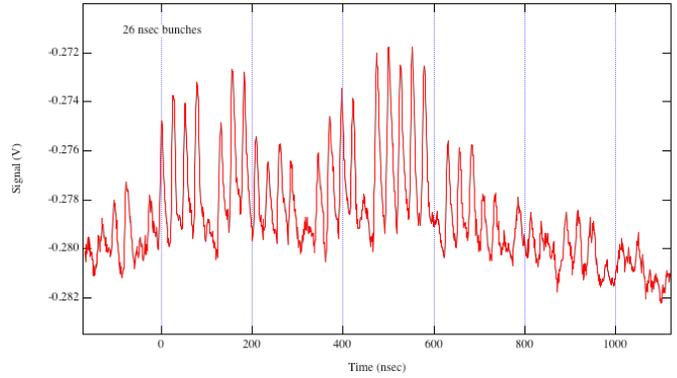

Figure 4.   Ionization chamber response with 25 ns bunch spacing

B. Beam tests at RHIC

The global operation of the device was validated during the RHIC Run 7 (100 GeV/c Au on 100 GeV/c Au). The detector was installed between the first and second module of the RHIC luminosity monitor (Zero Degree Calorimeter, ZDC). Results from dedicated vernier scans shown in Fig. 5 confirm a very satisfactory agreement between the event rates from the BRAN and the ZDC.
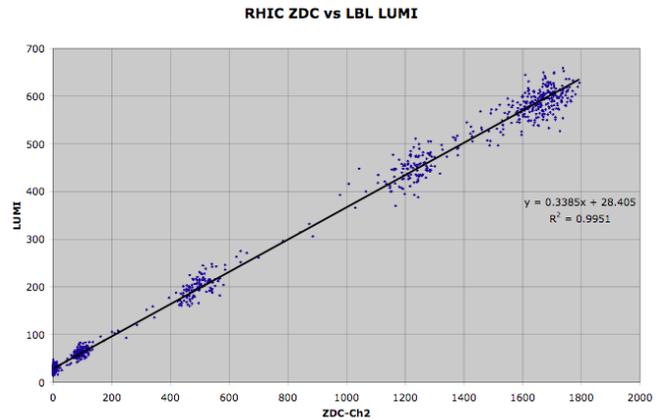

Figure 5.   Comparison between BRAN and ZDC rates in RHIC

C. Beam tests at the SPS

During the September 2008 test run at CERN the latest model of the BRAN detector was installed on the SPS H4 beamline. whose properties are collected in Table I.

Table I
H4 Beam Properties for the SPS Test Run

Energy	350 GeV
Particle	Protons
Distribution	Gaussian
Horizontal FWHM	0.805 mm
Vertical FWHM:	0.826mm

Using the nominal gas mixture (94%Ar + 6%N_2), voltage scans assessed the optimum combination of high voltage and gas pressure (200V/atm) at a working pressure of 8atm. The electron drift velocity as well as the signal amplitude were

optimized for maximum performance resulting in an amplifier rise time and gain of 50ns and 0.16μV/e^- respectively. Absorber scans were performed positioning Copper blocks in front of the ionization chamber with the incoming beam centered on a single quadrant of the detector. The detector's specifications and the variables used for the pulse height calculations are collected in Table II.

Table II
BRAN DETECTOR SPECIFICATIONS

Quadrant Area	4 x 16cm^2
Gap between Plates	6 x 1mm
Gas Type	94%Ar + 6%N$_2$
Gas Pressure	8 atm
$N'_{ion/mip}$	97.2e^+e^-/mip·cm·atm
e^- drift velocity	4.5cm/s
$(dE/dx)_{min}$ (Ar)	2.525·10^{-3}MeV/cm
Amplifier Gain:	0.16μV/e^-

IV. PULSE HEIGHT EVALUATION

The ionization chamber measures the energy deposition in six parallel-connected gas gaps. The conversion from energy deposition to the measured output (Volts) is derived hereafter assuming the chamber gaps are filled with pure Argon.
We define as MIP any particle carrying enough energy to ionize the gas and eventually produce positive or negative charges. The number of ionization pairs created per MIP can be calculated for any gas [3]. In our case:

$$N_{mip} = \frac{E_{Dep}}{l \ P \ (dE/dx_{min})_{Ar}} \quad (1)$$

where $(dE/dx_{min})_{Ar}$ is the minimum ionization energy in Argon per unit length and pressure [4]. The total number of electrons/positrons is determined from the total number of MIPs traveling trough the detector using the normalized value of $N'_{ion/mip}$ labeled in Table II. From (1):

$$Q_0 = l \ P \ N_{mip} \ N'_{ion/mip} \quad (2)$$

Assuming a uniform radiation of the detector area we introduce a 1/2 reduction factor for the actually collected charge Q to account for the center of gravity of the ionization process sitting in between the electrodes:

$$Q = \frac{1}{2} \ Q_0 \quad (3)$$

Taking into account further signal reductions caused by the Ballistic Deficit B_d and the cable attenuation λ the pulse height is:

$$U = Q \ \frac{g \ \lambda}{B_d} = \frac{g \ \lambda \ E_{Dep}}{2 \ B_d \ (dE/dx_{min})_{Ar}} \ N'_{ion/mip} \quad (4)$$

where g is the amplifier gain.
The amplifier used in the SPS tests ($g_{SPS} = 0.160\mu$V/e^-) is replaced by one with a better gain ($g_{LHC} = 0.224\mu$V/e^-) in the devices installed in the LHC.

V. SIMULATIONS

A. Beam Spread Analysis

Before implementing the actual BRAN geometry a beam spread analysis was performed to understand the actual size of the shower when it reaches the chamber. The H4 beam properties (Table I) were used as input for the simulations. The incoming beam position was centered on a 20cm thick Copper absorber with the same size as used in the tests. The shower size was analyzed through the energy deposition in a 10μm thick Copper layer at the end of the radiator. The 1.166cm FWHM of the profile of Fig. 6 confirms that the beam fits into a single quadrant of the detector.
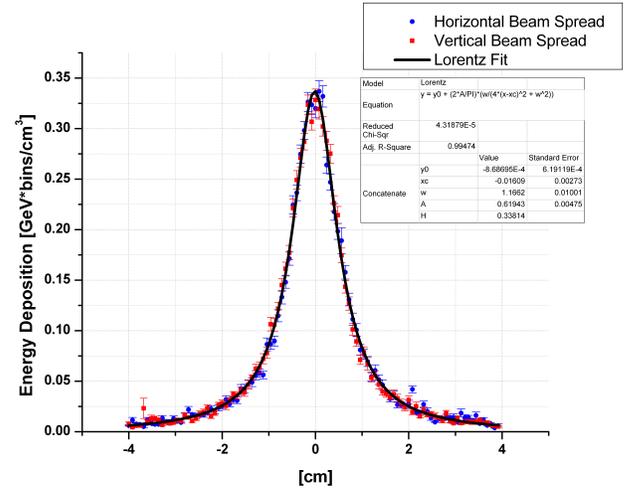

Figure 6. Energy deposition transverse spread inside a 10μm thick layer at the end of a 20cm thick Copper absorber. The 1.166cm FWHM confirms that the beam fits into a single quadrant of the detector.

B. SPS Geometry

A simplified version of the device was virtually constructed to simulate the beam energy deposition into the gas layers of a single quadrant of the BRAN detector. As shown in Fig. 7 the quadrants have been neglected and the BRAN structure was simplified to its stainless steel cover shielding and six 1mm Argon gaps separated by 2mm thick Copper layers.
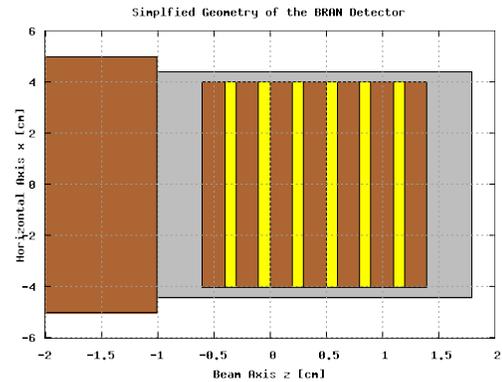

Figure 7. Simplified geometry of the BRAN detector. The six 1mm Argon gaps (yellow) are separated by 2mm thick Copper layers (brown), shielded by the stainless steel detector cover (grey). One absorber block is seen on the left side.

VI. Results & Analysis

A. Absorber Scan at the SPS

The results of the absorber scan performed at the SPS and the simulation data compared in Fig. 8 show an excellent agreement. As experimentally confirmed in the SPS test the shower maximum predicted from the simulation is around 20-25cm. The measured 5.31mV at shower maximum amplitude agrees well within the error bars with the simulation result (5.10± 0.02(stat.)± 0.96(syst.)mV). The main contribution to the systematic error comes from the Ballistic Deficit, varying between 2.4 and 3.0. The experimental data without absorber material in Fig. 8 show a higher offset compared to the simulation prediction. This offset appears to be constant throughout the measurement. Among the possible explanations for this feature are unexpected particle production in front of the detector such as particle collisions with the beam pipe, a longer distance between the end of the beam pipe and the detector or other systematic features which were not taken into account for in the simulation. Experimental and simulated data also agree well with the data taken at a previous test [5] performed at the SPS with 300GeV beam energy and a slightly different detector design. However, scaling the result of 4.4mV up to 350GeV one would expect the signal at shower maximum around 5.1mV.
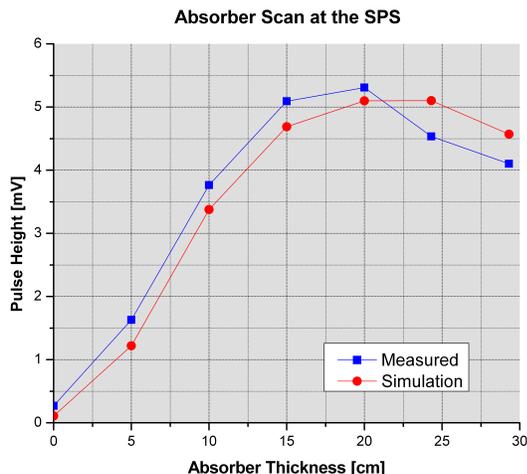

Figure 8. Measured (blue squares) and simulated (red dots) data from the absorber scan experiment.

In total 390 mips were produced and contributed to the signal. This corresponds to an energy deposition of 4.7MeV in the gas layers. The table of shower particles from the previous test in [5] was also reproduced. As it can be seen in Table III the simulation predicts a slightly smaller value of the mean energy per particle per proton but the total energy for each particle type is well reproduced.

B. BRAN in the TAN absorber

The setup of the BRAN detector simulated for the LHC is different from the SPS experimental setup.
A higher amplifier gain ($g = 0.224\mu$V/e^-) was used and the cable attenuation adjusted to $\lambda = 0.73$. We're implementing

Table III
THE FLUX AND MEAN ENERGY OF SHOWER PARTICLES PER 350GeV PROTON AT A DEPTH OF 20CM IN Cu. THE TOTAL ENERGY IS COMPARED TO THE PREVIOUS TEST RESULTS.

Particle Type	Flux [par./p]	Mean Energy [MeV]	Total Energy [GeV] Current	Previous
e^-	119.0	54	6.4	6.2
e^+	72.5	88	6.4	6.0
π^-	8.5	3545	30.1	26.9
π^+	8.1	4163	33.7	36.7
K^-	0.4	6967	2.9	3.4
K^+	0.8	5866	4.6	5.0
p	6.6	23311	153.9	121.7
n	27.7	671	18.6	33.5
γ	1098.1	26	28.2	25.0

this model in preparation for LHC beam operations and plan to study the detector performance for various LHC beam energy conditions.

VII. Conclusion

We have confirmed with exhaustive simulations a complete set of experimental measurements that validate the design and the expected performance of the BRAN luminosity detector. The good agreement between modeled and measured performance provides encouraging results in preparation of the upcoming LHC operation.

VIII. Acknowledgments

References

[1] A. Ferrari, P.R. Sala, A. Fasso, J. Ranft, "FLUKA: a multi-particle transport code.", CERN 2005-10, INFN/TC-05/11,SLAC-R-773,2005.
[2] V.Vlachoudis "FLAIR: A Powerful But User Friendly Graphical Interface For FLUKA" Proc. Int. Conf. on Mathematics, Computational Methods & Reactor Physics (M&C 2009), Saratoga Springs, New York, 2009.
[3] W.C. Turner, "Luminosity Instrumentation for the Absorbers in the Low β^* Insertions of the LHC", IEEE Trans.Nucl.Sci., Vol. 50, LBNL, 1999.
[4] C. Amsler et al. (Particle Data Group), Phys. Lett. B667, 1 (2008) and 2009 partial update for the 2010 edition.
[5] P. Datte et al., "Initital Test Results of an Ionization Chamber Shower Detector for a LHC Luminosity Monitor", IEEE Trans.Nucl.Sci., Vol. 50: 258-262, 2003.